Biosensors and Bioelectronics 25 (2010) 1160–1165

Contents lists available at ScienceDirect

Biosensors and Bioelectronics

journal homepage: www.elsevier.com/locate/bios

Iron oxide/carbon black (Fe_2O_3/CB) composite electrode for the detection of reduced nicotinamide cofactors using an amperometric method under a low overpotential

Yang Hee Kim [a], Taeho Kim [a], Ji Heon Ryu [b], Young Je Yoo [a,*]

[a] School of Chemical and Biological Engineering, Seoul National University, Seoul 151-744, Republic of Korea
[b] Graduate School of Knowledge based Technology and Energy, Korea Polytechnic University, Siheung, Gyeonggi 429-923, Republic of Korea

ARTICLE INFO

Article history:
Received 24 June 2009
Received in revised form 1 October 2009
Accepted 5 October 2009
Available online 14 November 2009

Keywords:
Amperometric detection
Dehydrogenase
Direct oxidation
Iron oxide/carbon black composite electrode
Nicotinamide cofactor

ABSTRACT

An amperometric biosensor for the detection of the reduced nicotinamide cofactors NADH and NADPH was designed, based on the electrochemical oxidation of NAD(P)H with an iron oxide/carbon black composite (Fe_2O_3/CB) electrode. The electrode exhibited excellent performances in that it led to a substantial decrease in the overpotential of electrochemical NADH oxidation. Iron oxide plays a significant role as a catalyst for NADH oxidation and the reaction occurs at +0.00 V (vs. Ag/AgCl). The method of the sensor construction is very simple and the sensor performed well, giving high sensitivity, high stability, and a broad detection range. The sensitivity of this system is 2.54 μA mM^{-1} and the limit of detection (S/N = 3) is 10 μM. A linear range was observed between 10 μM and 1000 μM of NADH (R^2 = 0.993), which is preferable to that of the previous studies. The Fe_2O_3/CB electrode also oxidizes NADPH under the same condition and can be applied as an NADPH sensor. Moreover, when the sensor system was integrated into a dehydrogenase-based sensor system, it also showed a good sensing performance.

1. Introduction

In the recent decades, nicotinamide cofactors such as reduced nicotinamide adenine dinucleotide (NADH) or reduced nicotinamide adenine dinucleotide phosphate (NADPH) have received a considerable interest because these cofactors are essential in hundreds of dehydrogenase reactions, including the biological electron transfer system used by all living organisms. Particularly, measuring NADH is very important because NAD(P)$^+$ is used as a cofactor for about 250 NAD^+-dependent and 150 $NADP^+$-dependent dehydrogenases. It can be applied to analytical detection, fermentation, clinical practices, food industry, and dairy industry. Therefore, the development of a detection system for NAD(P)H is attractive (Lobo et al., 1997).

Since the detection of many important biological analytes is carried out using an electrochemical method, a highly sensitive amperometric sensor is desirable. The direct oxidation of NADH on bare electrode surfaces, however, usually requires a high overpotential and suffers from a poor sensitivity. In fact, conventional electrodes such as carbon, gold, and platinum require an overpotential higher than +1.00 V (Jaegfeldt, 1980; Moiroux and Elving, 1978; Samec and Elving, 1983), which causes undesirable side reactions, remarkably increased background currents, hence, difficulties in obtaining accurate signals. In addition, the direct oxidation of NADH brings about fouling on the electrode surface due to undesirable dimer formations from the intermediates. Therefore, various mediators such as organic dyes (Kumar and Chen, 2007; Maroneze et al., 2008; Zhang and Gorski, 2005; Zhu et al., 2007), thio-substituted nucleobases (Behera and Raj, 2007), transitional metal complexes (Wu et al., 1996), and conducting polymers (Bartlett and Simon, 2003) have been employed for the purpose of decreasing the overpotential and the electrode fouling. However, although the use of such mediators seems promising, they still cause problems such as leakages from the electrode surface, lack of a long-term stability, and toxicity, which have a negative influence on their analytical applications.

Today, with the development of material science, there have been various trials to employ new materials, such as modified carbon electrodes (Campbell and Rishpon, 2001; Prasad et al., 2007) and nanomaterials (Deng et al., 2008; Liu et al., 2008; Zhang et al., 2004). The use of carbon nanomaterial electrodes is of great interest due to their unique structural and electrical properties. Carbon nanotubes (CNT) have wholly activated surfaces and oxygen-containing activated sites that are ideal for the immobilization of enzymes. Carbon nanofibers (CNF) are also used for biosensor electrodes because of their structural advantages for the electrocatalysis of biological molecules. Additionally, various materials such as gold nanoparticle multilayers and Ti-MCM (Dai et

* Corresponding author. Tel.: +82 2 880 7411; fax: +82 2 887 1659.
E-mail address: yjyoo@snu.ac.kr (Y.J. Yoo).

0956-5663/$ – see front matter © 2009 Elsevier B.V. All rights reserved.
doi:10.1016/j.bios.2009.10.004

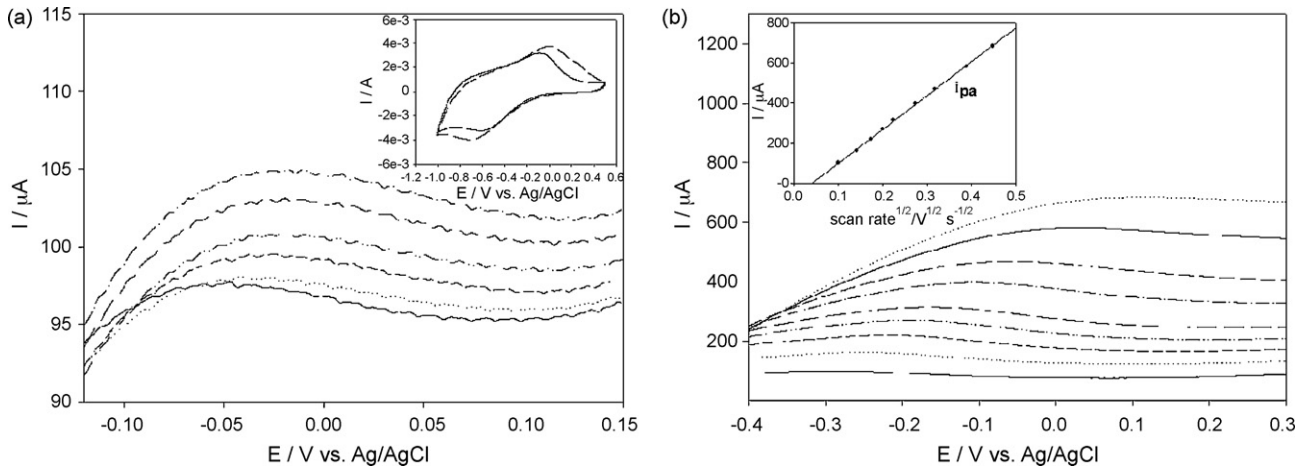

Fig. 1. (a) Linear sweep voltammograms of the Fe_2O_3/CB electrode with different NADH concentrations (0 mM, 1 mM, 2 mM, 3 mM, 4 mM, and 5 mM; arranged from bottom to top, respectively) (insert: cyclic voltammograms in the absence and presence of 1 mM NADH) at a scan rate of 50 mV s^{-1}; (b) linear sweep voltammograms of the Fe_2O_3/CB electrode at a scan rate of 10 mV s^{-1}, 20 mV s^{-1}, 30 mV s^{-1}, 40 mV s^{-1}, 50 mV s^{-1}, 75 mV s^{-1}, 100 mV s^{-1}, 150 mV s^{-1}, and 200 mV s^{-1}; arranged from bottom to top, respectively (insert: dependence of the peak current on scan rate) in pH 7.5 potassium phosphate buffer (100 mM).

al., 2007) were employed to decrease the high overpotential and minimize the effect of the electrode surface fouling.

Here, we report a new sensor for the nicotinamide cofactor detection based on the amperometric method. To overcome the limitations of previous studies, an iron oxide/carbon black composite (Fe_2O_3/CB) electrode was introduced for NAD(P)H oxidation under a very low overpotential without the employment of the mediators or chemical treatment. In our previous study, we found that direct electrochemical NAD(P)H oxidation is possible using a metal oxide electrode (Kim and Yoo, 2009). A metal oxide electrode including iron oxide has a role of an electrocatalyst for the NAD(P)H oxidation. Based on the previous results, we are able to detect NADPH as well as NADH. In addition, the proposed system can be applied to the ethanol detection by using NAD^+-dependent alcohol dehydrogenase.

2. Experimental

2.1. Reagents

Super P® conductive carbon black (CB) was obtained from TIMCAL graphite & carbon (Bodio, Switzerland) and polytetrafluoroethylene (PTFE) was kindly offered from the electrochemical energy conversion and storage laboratory in SNU. Iron oxide (Fe_2O_3), NAD^+, NADH, NADPH, and alcohol dehydrogenase from *Saccharomyces cerevisiae* (EC 1.1.1.1) were obtained from Sigma (St. Louis, USA). The reagents for buffer preparation were purchased from Junsei (Tokyo, Japan). Isopropanol and ethanol were obtained from Merck (Darmstadt, Germany). All reagents were used without further purification and aqueous solutions were prepared using deionized water from a Milli-Q water purification system (Millipore, France).

2.2. Apparatus

The surface of the prepared electrode was analyzed by SUPRA 55VP field emission scanning electron microscope (FE-SEM; Carl Zeiss, Oberkochen, Germany) with an accelerating voltage of 2 kV.

Electroanalytical measurements such as cyclic voltammetry, linear sweep voltammetry, and chronoamperometry were taken by using an Autolab PGSTAT 302N potentiostat/galvanostat (Eco Chemie, Utrecht, The Netherlands). This instrument was operated using the GPES program (Eco Chemie). Electrochemical impedance spectroscopy (EIS) was carried out using a CHI 660A electrochemical workstation (CH Instruments, Inc., Austin, USA). The EIS data were fit by Zview software. All electrochemical experiments were performed with a 5 mL reaction volume in a 20 mL electrochemical cell (Bioanalytical Systems, Inc., West Lafayette, USA). The electrode body (3 mm dia; BAS) filled with Fe_2O_3/CB or CB and a glassy carbon electrode (GC, 3 mm dia; BAS) was used as the working electrode. Platinum coil was used as the counter electrode and a RE-5B Ag/AgCl electrode (BAS) was used as the reference electrode.

The activity of alcohol dehydrogenase was determined by the change in absorbance of NADH at 340 nm using a Cary 50Conc UV–vis spectrophotometer (Varian, Victoria, Australia), the enzyme was put in 1 mM NAD^+ and 10 mM ethanol at 25 °C.

2.3. Preparation of the iron oxide/carbon black composite electrode

The Fe_2O_3/CB electrode was prepared for the NADH determination. The Teflon electrode body was previously cleaned by sonication with deionized water for 15 min. Iron oxide powder was mixed with carbon black at a given ratio (5:1, 10:1, and 15:1). For binding each component, a 0.1 mL PTFE dispersion in water (10 mg mL^{-1}) was used. The colloid was desiccated for 20 min, and carbon black and iron oxide were added on the dried colloidal PTFE. Using 2-propanol, the three components became mingled and kneaded until they were equally distributed. Then, the electrode body was filled with the mixed composite. Prior to every experiment performed with the composite electrode, the electrode was rinsed with deionized water.

3. Results and discussion

3.1. Characterization of the iron oxide/carbon black composite electrode

The iron oxide/carbon black composite (Fe_2O_3/CB) electrode was prepared for the amperometric detection of NAD(P)H. The surface distribution of Fe_2O_3 and CB on the surface of the prepared electrode was observed by FE-SEM (Supplementary data). It showed that the prepared electrode had a porous structure and that the composition materials for the electrode were well dispersed. The particle size of iron oxide was hundreds of nanometers and the average particle size of carbon black was approximately 30 nm.

The basic electrochemical properties of the Fe_2O_3/CB electrode were investigated by cyclic voltammetry and linear sweep voltam-

metry. The cyclic voltammograms of the prepared electrode were observed with and without NADH (Fig. 1(a, insert)). They showed the oxidation and reduction peak potentials in both cases. Using this electrode, NADH could be oxidized and reduced on the electrode surface directly. The anodic peak potentials of the electrode with and without NADH were +0.00 V and −0.09 V, respectively. The anodic peak potentials shifted toward positive 0.09 V and the anodic peak current was increased by adding NADH. These observations were also shown in the linear sweep voltammetric experiments. As shown in Fig. 1(a), the anodic current increased linearly with the increase in NADH concentration at +0.00 V. This infers NADH is well oxidized on the electrode and the electrode material has good properties for the construction of an NADH detection system. The applied potential for NADH oxidation (+0.00 V) is much lower than that in previous studies (Table 1).

In order to observe the kinetic characteristics of NADH oxidation by the Fe_2O_3/CB electrode, linear sweep voltammetry of the electrode was investigated with variable scan rates (Fig. 1(b)). The anodic peak current and the peak potential were shifted toward the positive direction by an increase in the scan rate. The change of the peak potential confirmed an electrochemical irreversibility of the reaction and whether the electrochemical NADH oxidation in this system was diffusion controlled.

The surface concentration of electroactive species (Γ) on the Fe_2O_3/CB electrode was determined by the relationship between I_p and Γ which can be estimated by the Laviron equation (Laviron, 1979):

$$I_p = \frac{n^2F^2\upsilon A\Gamma}{4RT} \quad (1)$$

where n is the number of electrons transferred, F the Faraday constant, υ the scan rate, A the electrode surface area, R the gas constant, and T the temperature. The surface coverage of the electroactive species of the Fe_2O_3/CB electrode was 0.187×10^{-10} mol cm^{-2}.

By AC impedance analysis, electron transfers between NADH and the Fe_2O_3/CB electrode were observed and compared with other controlled sets of electrodes, such as glassy carbon (GC) and carbon black (CB) electrodes (Fig. 2(a)). By the Nyquist plot, the value of charge-transfer resistance (R_{ct}) was estimated to be 239 Ω at the Fe_2O_3/CB electrode. It showed a semi-circle induced from the charge-transfer reaction at +0.00 V. However, capacitance by adsorption of ionic substances was only indicated for the GC and CB electrodes due to no charge-transfer reaction. In short, the charge-transfer reaction occurred on the Fe_2O_3/CB electrode but not on the GC and CB electrodes.

The mechanism of electrochemical NADH oxidation in the suggested system is as follows:

$$Fe_2O_3/CB + NADH \underset{k_{-1}}{\overset{k_1}{\rightleftarrows}} Fe_2O_3/CB \cdot NADH \xrightarrow{k_2} Fe_2O_3/CB + NAD^+ \quad (a)$$

$$Fe_2O_3/CB{\cdot}NADH \rightarrow Fe_2O_3/CB{\cdot}NADH^{\bullet+} + e^- \quad (b)$$

$$Fe_2O_3/CB{\cdot}NADH^{\bullet+} \rightarrow Fe_2O_3/CB{\cdot}NAD^{\bullet} + H^+ \quad (c)$$

$$Fe_2O_3/CB{\cdot}NAD^{\bullet} \rightarrow Fe_2O_3/CB{\cdot}NAD^+ + e^- \quad (d)$$

where NADH diffuses and adsorbs on the electrode surface, and then it is electrochemically oxidized by an ECE mechanism (a) (Moiroux and Elving, 1980; Kim and Yoo, 2009). According to the ECE mechanism, the first step of NADH electrochemical oxidation is an irreversible heterogeneous electron transfer. In this step, one electron is lost and a cation radical $NADH^{\bullet+}$ is produced (b). This step is shown to be rate-limiting in our system from the αn_a estimation. The value of an apparent transfer coefficient (α) was estimated using the shape factor equation and the Tafel analysis of the voltammogram. In an irreversible system, α could be calculated by the

Table 1
Comparison of the sensor performance for NADH detection.

Electrode	Electrode modified material	E_{appl} (mV vs. Ag/AgCl)	LOD (S/N = 3) (μM)	Linear range (μM)	Sensitivity	Remarks	Ref.
Mediated system							
GC	o-Aminophenol	+150	0.15	0.75–2.5	0.14 μA μM^{-1}		Nassef et al. (2006)
GC	Toludine blue/zinc oxide	+0	2.4	25–100	0.01 A M^{-1}		Kumar and Chen (2007)
SiO_2/TiO_2/graphite	Meldola blue	−120 (vs. SCE)	8	18–7290	0.58 μA mM^{-1}		Maroneze et al. (2008)
Au	Mercaptopyrimidine	+580	2.5	5–500	0.63 ± 0.005 μA μM^{-1} cm^{-2}	Square wave voltammetry	Behera and Raj (2007)
	4-Amino-2-mercaptopyrimidine		0.5		0.66 ± 0.008 μA μM^{-1} cm^{-2}		
GC	CNT/meldola blue	−100	0.048±0.02	Up to 500	0.52 ± 0.02 μA μM^{-1}		Zhu et al. (2007)
GC	CNT/azure-chitosan	−100	0.5	0.5–350	10.3 mA M^{-1}		Zhang and Gorski (2005)
GC	Poly(1,2-diaminobenzene) nanotubule	+450	n.d.	50–1000	99 nA mM^{-1}		Valentini et al. (2004)
Mediator-free system							
GC	CNT-chitosan	+400	3	5–300	130 ± 6 mA M^{-1} cm^{-2}		Zhang et al. (2004)
Activated carbon cloth	–	+100 (vs. SCE)	2	20–400	18 nA μM^{-1}		Campbell and Rishpon (2001)
CPE	CNFs	+450	0.02	0.02–11.47	10 nA μM^{-1}		Liu et al. (2008)
SPCE	–	+400	0.157	Up to 100	0.0915 μA μM^{-1}	Flow inject analysis	Prasad et al. (2007)
ITO	MWNTs/thionine/AuNPs	+200	0.1	0.5–237	17 nA μM^{-1}	w/o light	Deng et al. (2008)
			0.05	n.d.	115 nA μM^{-1}	w/light	
GC	Ti/MCM-41	+280 (vs. SCE)	8	10–1200	n.d.	Flow inject analysis	Dai et al. (2007)
Fe_2O_3/CB	–	**+0**	**10**	**10–1000**	**2.54 μA mM^{-1}**		**This study**

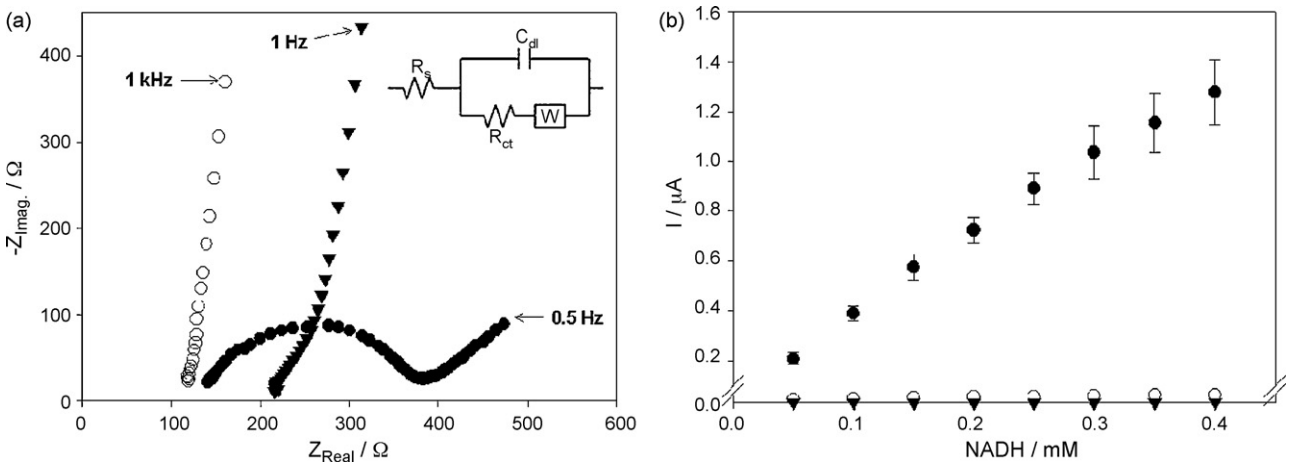

Fig. 2. (a) Nyquist plots for the Fe_2O_3/CB (●), GC (○), and CB (▼) electrodes in the presence of 1 mM NADH in pH 7.5 potassium phosphate buffer (100 mM). This experiment was performed using a frequency range of 0.5–5 kHz, +0.00 V, and 5 mV amplitude. (b) Calibration curve from the amperometric response of NADH at Fe_2O_3/CB (●), GC (○), and CB (▼) electrodes.

shape factor equation:

$$|E_p - E_{p/2}| = \frac{47.7}{\alpha n_a} \quad (2)$$

where n_a is the number of electrons transferred in the rate determining step, and the transfer coefficient value calculated is $\alpha n_a = 0.331$. Estimating αn_a from the Tafel plot revealed a similar value. A Tafel analysis was carried out using the following conditions: oxidation of 1 mM NADH was plotted as potential versus $\log_{10}$ current at pH 7.5, and a scan rate of 50 mV s^{-1}. A Tafel slope of 181 mV $decade^{-1}$ was obtained. According to the Tafel equation:

$$y = \frac{2.303RT}{\alpha n_a F} \quad (3)$$

where y is the Tafel slope. In addition, αn_a was calculated and a value of 0.327 was obtained, suggesting that in the overall reaction involving two electrons, the first electron transfer is the rate-limiting step (Banks and Compton, 2005; Moiroux and Elving, 1980). The neutral radical $NAD^{\bullet}$ was produced through a first-order deprotonation reaction of $NADH^{\bullet+}$ (c). A continual reaction for electron transfer from $NAD^{\bullet}$ occurred through a second heterogeneous electron transfer (d). This mechanism induced from ECE can be proved by current–voltage curves with different scan rates (Supplementary data). The NADH oxidation on the Fe_2O_3/CB electrode showed general characteristic of the ECE mechanism (Blaedel and Haas, 1970; Nicholson and Shain, 1965). To summarize the reaction mechanism briefly, the reduced form of the cofactor, NADH, diffuses and adsorbs onto the electrode surface. The cofactor is then electrochemically oxidized on the iron oxide via the ECE mechanism. The iron oxide has a role of an electrocatalyst in order to oxidize NADH and then it is reduced with formation of a metal-hydroxyl group from a metal-oxygen double bond. Then, the iron oxide is finally reoxidized to its original state, at which point it can again promote the oxidation of NADH (Supplementary data). The current variation by the electrons produced from this reaction can be detected as amperometric signals. The electron transfer rate (k_s) in this system can be estimated by the Laviron method using the calculated αn_a value of 2.61 s^{-1}.

As mentioned previously, the electrochemical NADH oxidation in this system is diffusion controlled. It was also confirmed by the linear relationship of the peak current with the square root of the scan rate. From the plot of this relationship, diffusion coefficient (D) can be estimated using the following equation:

$$I_p = (2.99 \times 10^5) A C_0 D^{1/2} \upsilon^{1/2} (\alpha n_a)^{1/2} \quad (4)$$

where A is the electrode surface area, C_0 the bulk concentration, υ the scan rate, and n the number of electrons transferred. αn_a is derived from Eqs. (2) or (3). The diffusion coefficient calculated from the slope of Fig. 1(b, insert) is 4.86×10^{-5} cm^2 s^{-1}.

3.2. Amperometric detection of nicotinamide cofactor

In an electrochemical analysis, the current difference from the electrocatalytic oxidation of NADH using the Fe_2O_3/CB electrode was observed. A chronoamperometric method was introduced to detect the current difference caused by NADH addition.

The effect of the electrode composition on sensing performance is shown in Fig. 2(b) by comparing the Fe_2O_3/CB electrode with the CB and GC electrodes, which do not contain iron oxide. GC is the most commonly used electrode. When the pure CB electrode was used, no response was observed because catalytic sites do not exist on the electrode surface at +0.00 V. In addition, an extremely low response was detected in the GC electrode system. This observation was also expected from the impedance result (Fig. 2(a)) that showed a charge-transfer on the Fe_2O_3/CB electrode but only increasing capacitance on GC and CB electrodes at +0.00 V.

In order to find the optimal composition at which the proposed electrode showed the largest response to NADH, the electrode composition of Fe_2O_3 and CB was varied and the current responses with different NADH concentrations were observed by amperometry at +0.00 V (Supplementary data). The best response occurred when a 10:1 composite electrode was used. The amperometric response did not show a linear correlation with the Fe_2O_3 weight. In this electrochemical system, Fe_2O_3 plays the role of an electrocatalyst for NADH oxidation while CB works as an electron carrier. Notably, the amount of CB is also critical for detecting electrochemical signals. Hence, it is not always important to have as high amounts of Fe_2O_3 as possible, without regarding the ratio to carbon black. This is because the electrons emitted from NADH oxidation cannot be efficiently transferred from the reaction to the detection system even though excess Fe_2O_3 catalytic sites exist for sufficient NADH oxidation. Therefore, it is highly important to make an electrode with a proper composition of Fe_2O_3 and CB.

To optimize the condition of NADH oxidation on the Fe_2O_3/CB electrode, amperometric experiments were performed at various pH levels (Supplementary data) from 7.0 to 9.0. At pH 7.5, the electrode showed the largest response to NADH.

Using the Fe_2O_3/CB (10:1) electrode, current changes with different NADH concentrations were observed by amperometric methods under the optimum condition for the NADH detection.

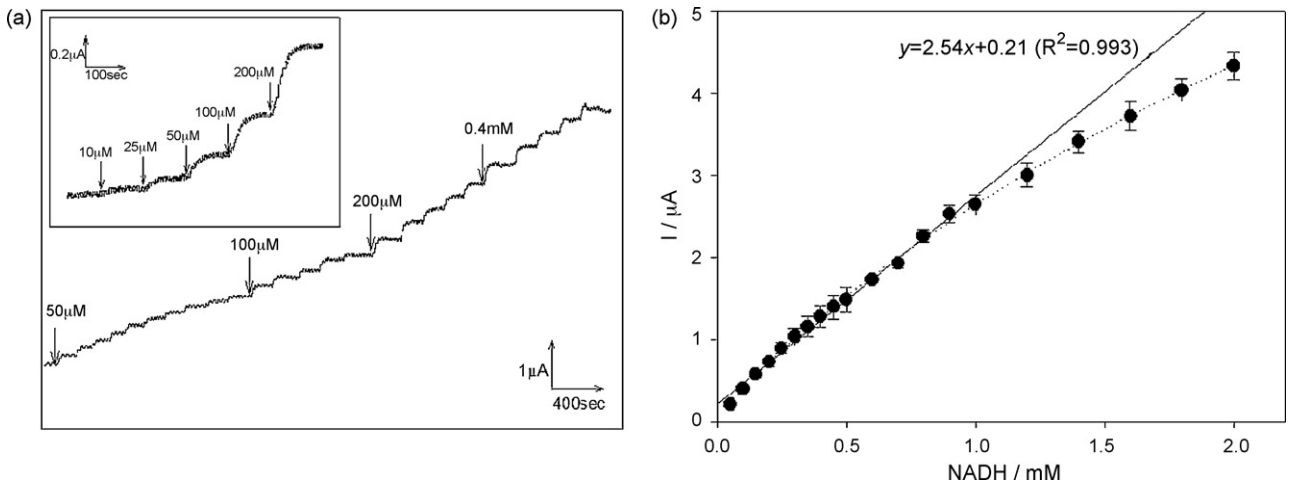

Fig. 3. (a) Amperometric response for NADH oxidation at the Fe_2O_3/CB electrode after addition of different NADH concentrations into a stirred solution of 100 mM potassium phosphate buffer (pH 7.5) at +0.00 V. (b) Calibration curve from the amperometric response of NADH.

Fig. 3(a) showed typical amperometric responses, time versus current, for NADH oxidation at +0.00 V. As NADH oxidized to NAD^+, the anodic current was increased. The time it took to reach a steady-state amperometric signal from NADH addition was less than 30 s. According to this amperometry, a linear range was observed between 10 μM and 1000 μM NADH (R^2 = 0.993), which is broader than the previous studies (Table 1). Moreover, there was a high sensitivity of 2.54 μA mM^{-1}. The limit of detection (LOD) of this sensing system, which is the minimum concentration at which the ratio of signal to noise is not less than 3, is 10 μM (S/N = 3).

The kinetic parameters of this reaction can be estimated by plotting the NADH concentration versus the current difference (Fig. 3(b)). This plot showed the kinetics of a heterogeneous second order reaction type, hence, the affinity of NADH for the electrode ($k_{-1} + k_2/k_1$ in (b)) can be estimated by a Michaelis–Menten constant (K_m) calculation; the value was 3.04 mM, deduced from a Lineweaver–Burk plot.

The effects of interferences that exist in typical biological systems with NADH, such as ascorbic acid and uric acid, were also investigated. The amperometric response of 0.1 mM NADH was not changed by adding 0.1 mM uric acid at +0.00 V. On the contrary, the amperometric response was increased toward the positive direction by the addition of 0.1 mM ascorbic acid. Although the signal from ascorbic acid was not for long and returned rapidly to the initial level of the current, it is important to reduce the effect of ascorbic acid in amperometry. This problem is caused from the antioxidant properties of ascorbic acid and might be solved by applying ascorbic oxidase, which oxidizes ascorbic acid selectively in the presence of oxygen (Pariente et al., 1997).

It has been known that conventional electrode fouling was caused by direct electrochemical oxidation of NADH and that it led to a reduction of the amperometric signals. To observe whether the electrode fouling occurs or not, 1 mM NADH was added and we measured the current change over time (Supplementary data). The current increase after NADH addition remained constant and the increased current lasted longer than 70 min without a decrease. If the electrodes were fouled, the amperometric signal by NADH oxidation would be reduced due to a decrease in the number of active sites for NADH oxidation. Based on this data, we can conclude that undesirable dimers from the intermediates were not formed and consequently, electrode fouling did not occur from the oxidation of NADH (Wang et al., 1998). The operational stability and storage stability were also observed. The electrode was exposed to continuous electrochemical polarization for 1 h every day, and then kept at 4 °C for storage. The amperometric response lowered by 10% after 7 days. The amperometric response maintained 89% of its initial value when the Fe_2O_3/CB electrode was stored at 4 °C without electrochemical polarization for 53 days. It showed a high operational stability and storage stability.

The prepared composite electrode can also be used for the amperometric analysis of another nicotinamide cofactor, NADPH (Supplementary data). The electrode showed a good sensing performance in detecting NADPH although the sensitivity was lower than that for NADH. Therefore, the Fe_2O_3/CB electrode can be applied for detection of NADH and NADPH, as well as for detection of other chemicals via utilizing enzyme mediated NADH and NADPH oxidation.

3.3. Ethanol biosensor based on the iron oxide/carbon black composite electrode with alcohol dehydrogenase

The previous results show that the potential at which the Fe_2O_3/CB electrode directly oxidizes a nicotinamide cofactor is +0.00 V and this system is applicable for an amperometric biosensor. By introducing the NAD(P)H sensing system to dehydrogenase reactions, biosensors can be designed to detect a certain chemical analyte that is used as a substrate of the dehydrogenase reaction. In this study, an ethanol biosensor was constructed as a model system and NAD^+-dependent alcohol dehydrogenase was used for ethanol oxidation. Ethanol is oxidized to acetaldehyde by the alcohol dehydrogenase in the presence of NAD^+ as a cofactor, which is reduced to NADH simultaneously. From the current change due to the NADH production from the enzyme reaction, the amount of ethanol consumed can be estimated. To optimize the ethanol detection, the amperometric response was observed at different pH levels (Fig. 4(a)). The maximum activity of the enzyme was obtained at pH 9.0. On the other hand, the maximum NADH response by electrochemical oxidation was seen at pH 7.5. When the electrochemical oxidation system was combined with the alcohol dehydrogenase reaction, the largest amperometric response was observed for ethanol detection at pH 7.5. Even though a high enzyme activity with high NAD^+ reduction was shown, the electrochemical NADH oxidation rate was not high enough to detect at pH 9.0. Accordingly, the NADH oxidation was rate limiting for the detection of ethanol in this system. The calibration curve of the ethanol sensor is shown in Fig. 4(b). It demonstrates that the response increases linearly with the concentration of ethanol from 0 mM to 1.5 mM (R^2 = 0.999). The sensitivity of this system was 0.94 μA mM^{-1} cm^{-2}. The sensing performance is almost similar or lower than existing ethanol sensors (Dai et al., 2007; Manso et al.,

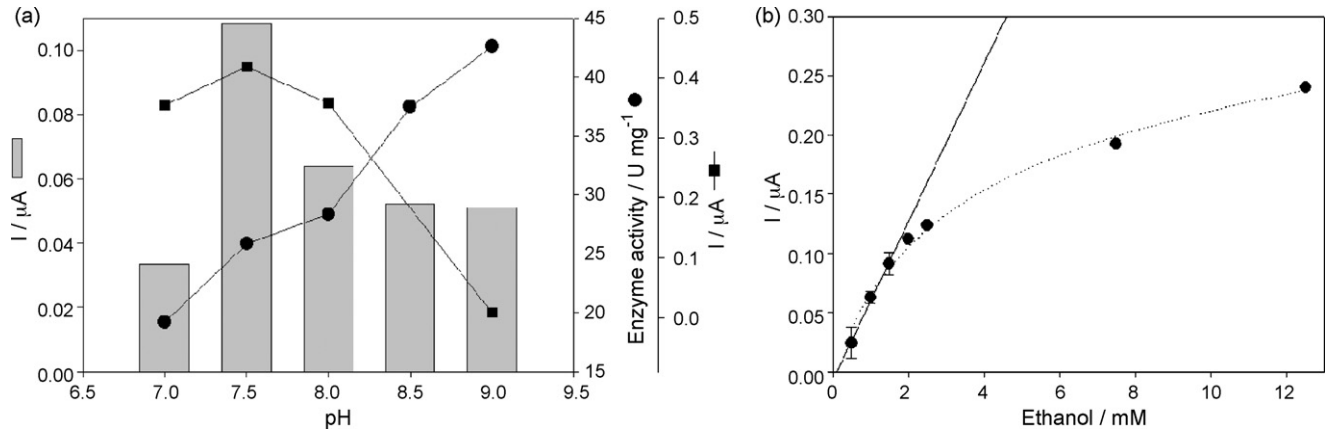

Fig. 4. (a) Effect of pH on the amperometric response to NADH oxidation (■), activity of alcohol dehydrogenase (●), and the amperometric response of the ethanol biosensor system (gray bar). (b) Calibration curve of the Fe_2O_3/CB electrode after addition of ethanol into a stirred solution that contained 2 mg alcohol dehydrogenase and 10 mM NADH in pH 7.5 potassium phosphate buffer at +0.00 V.

2008; Manesh et al., 2008; Santos et al., 2003, 2006; Tsai et al., 2007; Wu et al., 2007). However, our system has a big advantage that it can analyze ethanol under a very low overpotential without a mediator. The reaction condition for the ethanol detection is not yet optimized, hence, the performance can be improved by considering the concentration of enzyme, cofactor, and composition of electrolyte. Anyhow, the suggested NADH detection system clearly has broad applications in the construction of various dehydrogenase-based biosensors.

4. Conclusion

An iron oxide/carbon black (Fe_2O_3/CB) electrode was prepared and used for the sensor fabrication. The reduced forms of two nicotinamide cofactors, NADH and NADPH, can be electrochemically oxidized by the Fe_2O_3/CB electrode. Iron oxide has the catalytic activity for the NAD(P)H oxidation and carbon black has the role of an electron carrier in this system. Using the Fe_2O_3/CB electrode, we developed an amperometric biosensor for the detection of NAD(P)H. The most distinguishable finding is that the sensor showed its function under a very low overpotential, +0.00 V without a mediator. It also showed a good sensor performance such as a high sensitivity, a broad linear range, and a good stability. Moreover, electrode fouling, which generally occurred in direct NADH electrochemical oxidation, was not observed in our system. The suggested amperometric detection system for NAD(P)H was applied as an ethanol biosensor and it showed a good sensor performance. Thus, this study suggests that the Fe_2O_3/CB electrode is a promising candidate for sensor design. By employing electrochemical oxidation coupled with the enzyme reaction system, various kinds of chemicals can be detected.

Appendix A. Supplementary data

Supplementary data associated with this article can be found, in the online version, at doi:10.1016/j.bios.2009.10.004.

References

Banks, C.E., Compton, R.G., 2005. Analyst 130, 1232–1239.
Bartlett, P.N., Simon, E., 2003. J. Am. Chem. Soc. 125 (14), 4014–4015.
Behera, S., Raj, C.R., 2007. Sens. Actuators B: Chem. 128 (1), 31–38.
Blaedel, W.J., Haas, R.G., 1970. Anal. Chem 42 (8), 918–927.
Campbell, C.E., Rishpon, J., 2001. Electroanalysis 13 (1), 17–20.
Dai, Z., Lu, G., Bao, J., Huang, X., Ju, H., 2007. Electroanalysis 19 (15), 1591–1596.
Deng, L., Wang, Y., Shang, L., Wen, D., Wang, F., Dong, S., 2008. Biosens. Bioelectron. 24 (4), 951–957.
Jaegfeldt, H., 1980. J. Electroanal. Chem. 110 (1–3), 295–302.
Kim, Y.H., Yoo, Y.J., 2009. Enz. Microb. Tech. 44 (3), 129–134.
Kumar, S.A., Chen, S.-M., 2007. Electroanalysis 19 (18), 1952–1958.
Laviron, E., 1979. J. Electroanal. Chem. 101, 19–28.
Liu, Y., Hou, H., You, T., 2008. Electroanalysis 20 (15), 1708–1713.
Lobo, M.J., Miranda, A.J., Tuñón, P., 1997. Electroanalysis 9 (3), 191–202.
Manesh, K.M., Santhosh, P., Gopalan, A., Lee, K.P., 2008. Talanta 75 (5), 1307–1314.
Manso, J., Mena, M.L., Yáñez-Sedeño, P., Pingarrón, J.M., 2008. Electrochim. Acta 53 (11), 4007–4012.
Maroneze, C.M., Arenas, L.T., Luz, R.C.S., Benvenutti, E.V., Landers, R., Gushikem, Y., 2008. Electrochim. Acta 53 (12), 4167–4175.
Moiroux, J., Elving, P.J., 1978. Anal. Chem. 50, 1056–1062.
Moiroux, J., Elving, P.J., 1980. J. Am. Chem. Soc. 102 (21), 6533–6538.
Nassef, H.M., Radi, A.-E., O'Sullivan, C.K., 2006. Electrochem. Commun 8 (11), 1719–1725.
Nicholson, R.S., Shain, I., 1965. Anal. Chem 37 (2), 178–190.
Pariente, F., Tobalina, F., Moreno, G., Hernandez, L., Lorenzo, E., Abruna, H.D., 1997. Anal. Chem. 69 (19), 4065–4075.
Prasad, K.S., Chen, J.C., Ay, C., Zen, J.M., 2007. Sens. Actuators B: Chem. 123 (2), 715–719.
Samec, Z., Elving, P.J., 1983. J. Electroanal. Chem. 144 (1–2), 217–234.
Santos, A.S., Freire, R.S., Kubota, L.T., 2003. J. Electroanal. Chem. 547 (2), 135–142.
Santos, A.S., Pereira, A.C., Duran, N., Kubota, L.T., 2006. Electrochim. Acta 52 (1), 215–220.
Tsai, Y.-C., Huang, J.-D., Chiu, C.-C., 2007. Biosens. Bioelectron. 22 (12), 3051–3056.
Valentini, F., Salis, A., Curulli, A., Palleschi, G., 2004. Anal. Chem 76 (11), 3244–3248.
Wang, J., Pamidi, P.V.A., Jiang, M., 1998. Anal. Chim. Acta 360 (1–3), 171–178.
Wu, Q., Maskus, M., Pariente, F., Tobalina, F., Fernandez, V.M., Lorenzo, E., Abruna, H.D., 1996. Anal. Chem. 68 (20), 3688–3696.
Wu, L., Zhang, X., Ju, H., 2007. Anal. Chem. 79 (2), 453–458.
Zhang, M., Gorski, W., 2005. Anal. Chem. 77 (13), 3960–3965.
Zhang, M., Smith, A., Gorski, W., 2004. Anal. Chem. 76 (17), 5045–5050.
Zhu, L., Zhai, J., Yang, R., Tian, C., Guo, L., 2007. Biosens. Bioelectron. 22 (11), 2768–2773.